Data-Driven Aeroacoustic Modelling: Trailing-Edge Noise

Data-Driven Aeroacoustic Modelling: Trailing-Edge Noise

Renzo Arina* and Andrea Ferrero.†
Dept. of Mechanical and Aerospace Eng., Politecnico di Torino, Torino, Italy

Broadband noise emitted at the trailing edge of an airfoil represents a significant contribution to the noise emission in rotors, wind turbine and fan blades, in low Mach number flows. High-fidelity calculations are out of the scope when fast parametric calculations are needed. In these cases it is necessary to resort to analytical models and the most popular one is the model proposed by Amiet. In the model, the knowledge of the wall pressure spectrum allows to define an equivalent point source located at the trailing edge. The description of the turbulent wall pressure spectrum is of major importance for the correct noise prediction. Proposed empirical laws of wall pressure spectra in presence of adverse pressure gradients are limited to cases which are not too far from the test cases employed for their calibration.

Recently, the development of machine learning techniques make it possible to analyze large amounts of experimental data in order to automatically extract modeling knowledge. However measurements of pressure fluctuations near a trailing edge are difficult. An alternative solution is to measure the far-field trailing-edge noise at each condition. The measures are comparatively simpler and contain all the information about the source.

In this work a deep learning algorithm, based on a standard feed-forward Artificial Neural Network (ANN) and a Random Forest (RF) algorithm are applied to far-field directivity data sets. The motivation of the present work is to evaluate the prediction ability of the ANN and RF models. The proposed approach allows to build a general model which can potentially be trained on experimental data and so it is not limited by the simplifying assumptions required by analytical models or empirical wall pressure spectrum.

The prediction capabilities of ANN and RF are investigated by considering data not included in the training database. The potential of RF regression for the evaluation of the prediction uncertainty is also addressed. The proposed models are based on a splitting in sub models: the ANN or the RF algorithm is used to describe the noise directivity while a polynomial model is introduced for the prediction of the emitted acoustic power. This splitting, which improves significantly the training performance, can be seen as a possible way to introduce a physical constraint to the machine learning model which is forced to satisfy a constraint on the emitted power. The proposed procedure is tested on an artificial database generated by the Amiet model. However, it can be directly applied to experimental data or high-fidelity calculations.

I. Introduction

Flow noise reduction is an important issue in the design of many industrial applications and the development of efficient computational models for the acoustic prediction is of major interest. Aeroacoustic computational tools must be reliable and also sufficiently fast if several parametric calculations are needed as in the case of design optimization. In presence of rotors and fan blades, in low Mach number flows, one source of noise is represented by the so-called trailing-edge noise, or airfoil self-noise [1, 2]. The broadband noise emission is associated with the sudden reorganization of the vortical motion when the turbulent boundary layer reaches the thin trailing edge. The corresponding pressure fluctuations partially induce density fluctuations which propagate as sound waves.

The problem of edge scattering has been addressed by Amiet [3, 4]. However, the prediction capability of the analytic Amiet model is limited since it is based on the thin-airfoil theory approximations. It does not take into account some features of the airfoil such as curvature and thickness. Statistically identical turbulent boundary layers are assumed to form on either side of the airfoil. The model provides the relationship between the boundary-layer pressure fluctuations and the trailing-edge noise. The knowledge of the wall pressure spectrum allows to define an equivalent point source located at the trailing edge. However, the boundary-layer turbulence is strongly dependent upon the airfoil geometry and

*Associate Professor, renzo.arina@polito.it, AIAA Senior Member.
†Assistant Professor, andrea_ferrero@polito.it, AIAA Member.

angle of attack, therefore the description of the turbulent wall pressure spectrum is of major importance for a correct noise prediction. Analytical models of wall pressure spectra for turbulent boundary layers, in presence of adverse pressure gradients, can be obtained as integral solutions of the Poisson equation for the incompressible pressure in the wavenumber-frequency domain [5]. However, such solutions present several numerical difficulties. An alternative approach, proposed already by Amiet [3], was to adopt an empirical turbulent wall pressure spectrum. Among several proposals, the empirical law of Goody [6] describes accurately boundary layers in absence of pressure gradient and accounts for Reynolds number effects. More recently the effect of pressure gradients have been introduced in the Goody's law [7–11], but the reliability of this empirical spectra is limited to cases which are not too far from the test cases employed for their calibration. To improve their reliability it would be necessary to measure turbulent pressure fluctuations for a wide range of airfoils and flow conditions.

Measurements of pressure fluctuations near a trailing edge are difficult, it is necessary to separate out the boundary-layer pressure fluctuations from the trailing-edge response. An alternative solution is to measure the far-field trailing-edge noise at each condition. The measures are comparatively simpler and contain all the information about the source. Brooks et al. [2] measured the trailing-edge noise over a large range of conditions and provided empirical correlations for airfoil trailing-edge noise. The Brooks, Pope and Marcolini (BPM) method is a tool widely used for fast, and quite reliable, predictions of airfoil self noise.

Recently, research efforts have been devoted to the development of Machine Learning (ML) techniques which make possible to analyze large amount of experimental data in order to automatically extract modelling knowledge. ML techniques have been applied in many fields, and in the context of fluid mechanics they have proved that can accurately interpolate between parametric flow data [12] or improve turbulence modelling [13]. ML is a vast field, amongst the numerous algorithms the most advanced and mature belong to the category of supervised learning methods. In a supervised learning algorithm, such as an Artificial Neural Network (ANN), a proper prediction model is constructed using an iterative training process which finds a map between some inputs and some outputs available in the database. With large amount of available training data, multilayer ANNs, belonging to the so-called deep learning, have solved complex applications [14]. Another important ML method is the Random Forest (RF) algorithm [15] in which multiple decision trees are grown in a random forest. Trees can capture complex structures in the data, and if grown sufficiently deep, have relatively low bias but they are usually noisy. The essential idea in RF is to average many noisy but unbiased models to reduce the variance.

The main objective of the present work is to assess the capabilities of ML algorithms to predict the trailing edge noise by training the model on a reduced amount of data. The training database is here generated by applying the Amiet model: however, the proposed methology is general and can be directly applied to experimental data.

Data-driven methods have been recently proposed for improving the Amiet model. The empirical wall pressure spectra discussed so far were partially tuned with data obtained from the solution of the Reynolds Averaged Navier-Stokes (RANS) equations. Data which may result inaccurate because of the limits of turbulence models. In the work of Wilsby and Sandberg [16] the data-driven method based on Gene Expression Programming (GEP) is used to improve the $k-\omega$ SST turbulence model, using high-fidelity simulations around a controlled diffusion airfoil. The improved turbulence model provide a better mean flow statistics used to define the wall pressure spectrum. Alternately, in the work of Dominique et al. [17] a GEP data-driven approach is used to directly built up an empirical wall pressure spectrum.

In both cases the attention is focused on the pressure fluctuations in the turbulent boundary layer. In this work, following the approach of Brooks et al. [2], the focus is on the far-field trailing-edge noise at each condition. The data-driven modelling, based on constrained ANN or RF, is used to choose the best architectures of ANN and RF which describe the sound directivity. The main objective of the work is to verify if the ANN and RF algorithms are able to reproduce the trailing-edge noise, the directivity, under different conditions of flow and geometrical conditions, and to investigate their minimum complexity. For the training it is necessary a database of acoustic far fields for a wide range of conditions. Experimental data are very rare and usually incomplete. Starting from the assumption that the extensions of the Amiet model [8, 9], even if they display several discrepancies, provide a reasonable representation of the phenomenon, the study is performed using an *artificial* database for the trailing- edge noise emitted by a NACA0012 airfoil in several working conditions. The data are generated using the empirical models for the wall pressure spectrum [8] and the Amiet theory for the acoustic propagation. The basic idea is that the artificial database, used to define the architecture of the ML algorithm, is not too far from the experimental results. In this way, the present study contributes to the definition of the complexity of a ML algorithm (ANN or RF) to be employed on experimental database or data provided by high-fidelity simulations.

In Section II a brief description of the Amiet's analytical model for trailing-edge noise is presented, with the improvements proposed by Rozemberg et al [8] and by Kamruzzaman et al. [9]. The results obtained by the two

models are compared in the case of the NACA0012 airfoil with experimental data [18] and the artificial database is described. Section III is devoted to the study of the two data-driven models, the ANN deep learning technique and the RF algorithms. Final conclusions are drawn up in section IV.

II. Analytical model for broadband trailing edge noise

Broadband trailing-edge noise is due to the scattering of the unsteady vortical structures of the boundary layers, on the pressure and suction side of a lifting surface, at the trailing edge. The acoustic problem can be tackled solving the Curle equation [19]. To overcome the difficulties encountered for the specification of the quadrupole source term, Amiet formulated the problem in terms of airfoil surface pressure. The basic assumption is that the turbulent velocity field is unaffected by the presence of the trailing edge and the turbulence is considered statistically steady. These assumptions allow to apply the wall pressure spectrum which would exist in the absence of the trailing edge. The boundary value problem is modeled by considering surface pressure disturbances traveling downstream of a semi-infinite flat plate in upstream direction [3, 4].

For a wing of high aspect ratio, the noise perceived by an observer located in the mid-span plane is described by the power spectral density for a given frequency ω and position $\mathbf{x} = (y = 0, R, \theta)$

$$S_{pp}(\mathbf{x}, \omega) = 2\left(\frac{\omega c z}{4\pi c_0 \sigma^2}\right) L \, |\, \mathcal{L}(\omega, \theta)\,|^2 \, \ell_y(\omega) \Phi_{pp}(\omega) \,, \tag{1}$$

where c is the chord, L the plate span, $\mathcal{L}(\omega, \theta)$ the aeroacoustic transfer function ([20], eq. 9), $\sigma^2 = x^2 + \beta^2(y^2 + z^2)$, $\beta^2 = 1 - M^2$ with M the Mach number of the uniform stream and c_0 the speed of sound in the undisturbed medium. $\ell_y(\omega)$ is the spanwise correlation length given by the Corcos model $\ell_y(\omega) = 1.2 U_c/\omega$, being U_c the convection velocity and $\Phi_{pp}(\omega)$ the wall pressure spectrum.

Formula (1) provides the scaling and directivity properties of the trailing-edge noise. A quantitative description requires an estimate of the wall pressure spectrum describing the turbulent structure of the boundary layer near the trailing edge. A semi-empirical normalised wall pressure spectrum is represented by the relation

$$\frac{\Phi_{pp}}{\Phi^*} = \frac{a \widetilde{\omega}^b}{(i\widetilde{\omega}^c + d)^e + \left(f R_T^g \widetilde{\omega}\right)^h} \,, \tag{2}$$

where $\widetilde{\omega} = \omega \delta^*/U_e$, $R_T = \delta^* \tau_w/(U_e \mu)$ and $\Phi^* = \tau_w^2 \delta^*/U_e$. δ^* is the boundary-layer displacement thickness and τ_w the wall shear stress in a position near the airfoil trailing edge. Defining the Zagarola-Smith parameter $\Delta = \delta/\delta^*$, the Clauser's equilibrium parameter $\beta_c = (\theta/\tau_w)(dp/dx)$ and the Coles' wake function $\Pi = 0.8(\beta_c + 0.5)^{3/4}$, in the Rozenberg model [8] the parameters are defined as: $a = [2.82\Delta^2(6.13 * \Delta^{-0.75} + d)^e][4.2\Pi/\Delta + 1]$, $b = 2.0$, $c = 0.75$, $d = 4.76(1.4/\Delta)^{0.75}(0.375e - 1)$, $e = 3.7 + 1.5\beta_c$, $f = 8.8$, $g = -0.57$, $h = min(3, 19/\sqrt{R_T}) + 7$, $i = 4.76$. In the Kamruzzaman [9] model the parameters are: $a = 0.45[1.75(\Pi/\beta_c)^{2m} + 15]$, $m = 0.5[(\delta^*/\theta)/1.31]^{0.3}$, $b = 2.0$, $c = 1.637$, $d = 0.27$, $e = 2.47$, $f = 1.15^{-2/7}$, $g = -2/7$, $h = 7$ and $i = 1$. The boundary-layer properties required by the models are evaluated by means of the XFoil tool [21]. The wall presure spectrum determines the magnitude of the noise source propagated by means of the Amiet expression (1).

Considering a rectangular wing of span $L = 1\,m$ with NACA0012 airfoil of chord $c = 0.4\,m$, at Reynolds number $Re = 1.5 \cdot 10^6$, at angle of attack $\alpha = 4°$, in Figure 1a is reported the 1/3 octave band far-field noise

$$L_{p(1/3)} = 10 \log_{10}(\mathcal{I}) = 10 \log_{10}\left(\frac{S_{pp}}{p_{ref}^2}\right) \,, \quad p_{ref} = 2\,10^{-5}\,\text{Pa} \,,$$

evaluated at $R = 1\,m$, $\theta = 90°$ from the trailing edge. The numerical results for the two wall pressure models are compared with the experimental data of IAG reported in [18]. In Figure 1b the sound intensity directivity $\mathcal{I}$, normalised with respect to p_{ref}^2, is shown.

The comparison indicates that the two models are more or less equivalent. It must be pointed out that the shape of the directivity plot depends only upon the transfer function $\mathcal{L}(\omega, \theta)$. The magnitude differences are due to the small differences of the predicted wall pressure spectra Φ_{pp} at the selected frequency. Therefore the artificial database, for the NACA0012 airfoil (chord $c = 0.4\,m$), at $\alpha = 4°$and $Re = 1.5\,10^6$, has been obtained with the Rozemberg model only. The main interest in the present work is to test the ability of the data-driven model to reproduce the directivity in shape and amplitude for a wide range of frequency. As can be seen in Figures 2, the number of lobes observed in the directivity

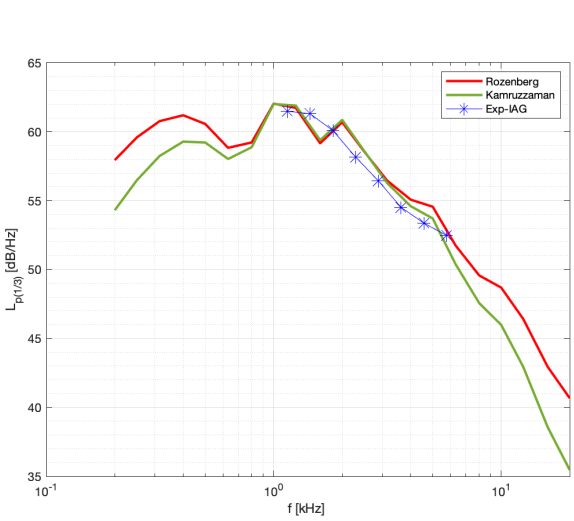

(a) Far field noise, $R = 1\,m$**,** $\theta = 90°$

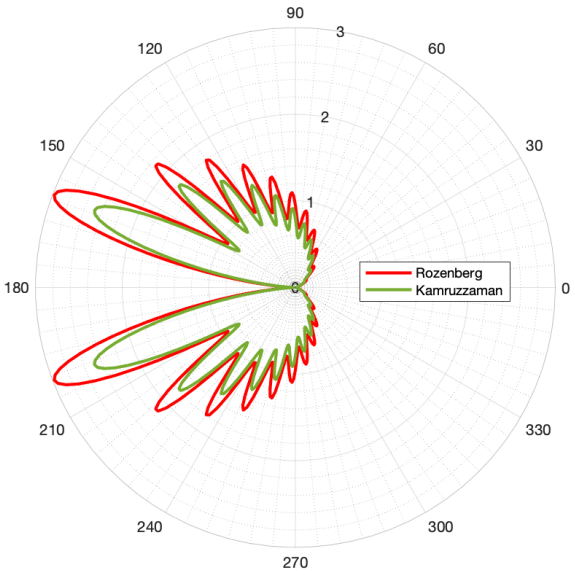

(b) Normalised directivity $\mathcal{I}$ **at** $R = 1\,m$**,** $f = 4500\,Hz$

Fig. 1 NACA0012, chord $c = 0.4\,m$**,** $\alpha = 4°$**,** $Re = 1.5 \cdot 10^6$

pattern is strongly related with the frequency. For a frequency of 100 Hz, the shape has a dipolar aspect (Figure 2a), while increasing the frequency more lobes appear, as in Figure 2b for 10000 Hz. Also the magnitude of the normalised directivity changes significantly with the frequency. The database is built up with 21 frequencies logarithmically equally spaced in the range $10^2 Hz < f < 10^4 Hz$ and a uniform sampling of the direction angle $0 < \theta < 2\pi$ (360 samples in θ). The database contains two inputs (logarithm of frequency f and direction θ) and one output (normalised directivity $\mathcal{I}$).

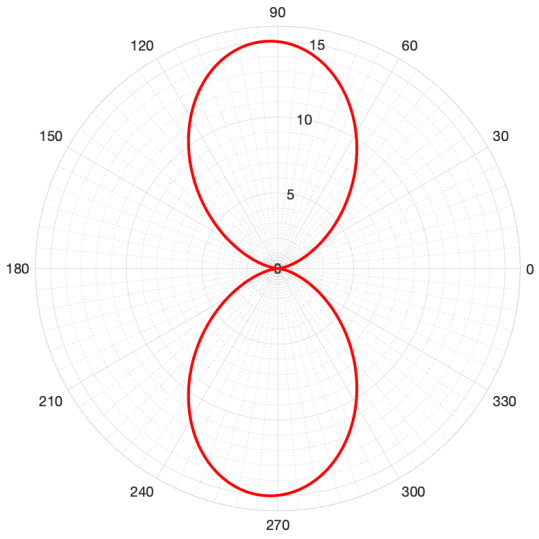

(a) $f = 100\,Hz$

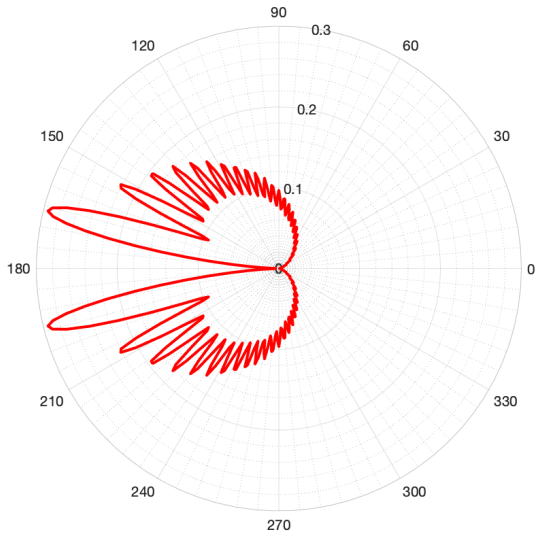

(b) $f = 10000\,Hz$

Fig. 2 Normalised directivity $\mathcal{I}$ **at** $R = 1\,m$

III. Machine learning on an artificial database

A. Unconstrained ANN model

First of all an ANN is trained on the artificial database without any normalisation of the data. Different ANN architectures are investigated and different sampling of the parameter space are evaluated. The ANN is trained by using the Matlab toolbox which randomly splits the database in a training set (75% of the data), a validation set (15% of the data) and a test set (10% of the data). The validation set is used to stop the training in order to avoid overfitting: the prediction error on the validation set does not contribute to the goal function which drives the training but, when it starts to increase, the training is stopped.

The magnitude of $\mathcal{I}$ changes significantly with the frequency. Furthermore, the number of lobes observed in the directivity pattern is strongly related with the frequency, as shown in Figures 2. This makes the training very difficult. In Figure 3 the directivity pattern at $f = 4500$ Hz predicted by a standard feed-forward ANN with sigmoid activation functions is reported: the network has 16 hidden layers and 10 neurons per hidden layer. The architecture was chosen after a preliminary study on a similar database [22]. A comparison with the reference solution, which is not included in the training database (the closest values are 3981.07 Hz and 5011.87 Hz) shows that the ANN produces a large prediction error. This behaviour is expected because ANNs performs poorly when the input and output variables are not properly scaled. Similar behaviours are also observed changing the architecture of the ANN, that is the number of hidden layers and number of neurons, or changing the sampling of the database.

B. Power-constrained ANN model

The results reported in the previous section suggest that a normalisation should be introduced in the database before performing the training. Among several possibilities, a normalisation with a clear physical meaning is investigated in this work. In particular, the database is pre-processed in order to evaluate the integral I of the $\mathcal{I}$ on all the directions:

$$\mathrm{I}(f) = \int_0^{2\pi} \mathcal{I}(f, \theta')\, d\theta' \,. \tag{3}$$

This integral could be evaluated analitycally starting from the solution provided by Amiet which is used to generate the database. However, the goal of this work is to develop a procedure which can be applied on experimental data: for this reason the integral is evaluated numerically by means of the trapezoidal rule.

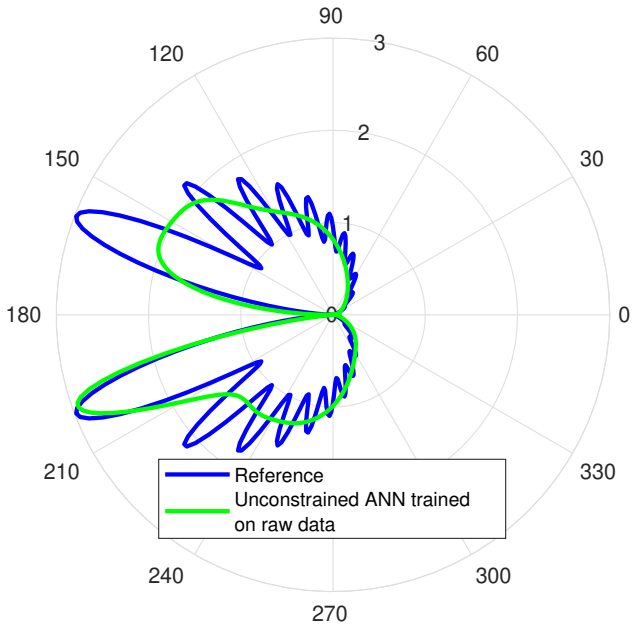

Fig. 3 Directivity pattern predicted by unconstrained ANN at 4500 Hz

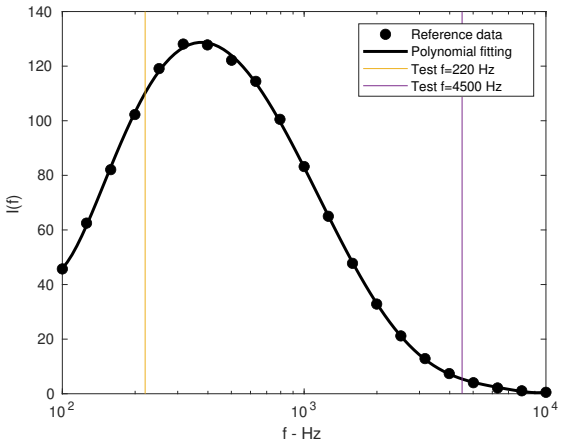

Fig. 4 Polynomial fitting of $\mathrm{I}(f)$ for the finest database (20 intervals in the frequency range $10^2 - 10^4$ Hz)

The database is then pre-processed by normalising the $\mathcal{I}$ pattern with respect to $\mathrm{I}(f)$:

$$\tilde{\mathcal{I}}(\theta, f) = \frac{\mathcal{I}(\theta, f)}{\mathrm{I}(f)} \ . \tag{4}$$

In this way the integral of the new variable $\tilde{\mathcal{I}}$ is always unitary: this improves significantly the performance of the ANN because now it is trained on directivity patterns which share the same range.

The ANN trained with the normalised data is able to perform accurate predictions for frequencies not included in the training database. However, the output of the network provides the normalised variable $\tilde{\mathcal{I}}$. In order to predict $\mathcal{I}$, it is necessary to introduce a second model which allows to approximate the function $\mathrm{I}(f)$ for frequencies not included in the training database. This is done by performing polynomial regression on the values of $\mathrm{I}(f)$ available in the database. In order to get better scaling the polynomial independent variable is not the frequency but its logarithm. The plot in Figure 4 shows the training data and the polynomial $\mathrm{I}_p(\log(f))$.

As a result, the $\mathcal{I}(\theta, f)$ is predicted as:

$$\mathcal{I}(\theta, f)_{ANN} = \frac{\mathrm{I}_p(\log(f))}{\int_0^{2\pi} \tilde{\mathcal{I}}_{ANN}(\theta', \log(f))d\theta'} \tilde{\mathcal{I}}_{ANN}(\theta, \log(f)) \ . \tag{5}$$

In this way there are two benefits: first of all, the training of the ANN is more accurate because of the normalisation. Secondly, the model $\mathrm{I}_p(\log(f))$ controls the total acoustic power emitted by the trailing edge at the different frequencies: the polynomial model introduces a correction factor in order to scale the ANN prediction. In this framework, it is possible to see the polynomial model as a physical constraint which is imposed to the ANN model.

A prediction for $f = 4500$ Hz, not included in the training database, with an ANN characterised by 16 hidden layers and 10 neurons per layer is reported in Figure 5.

The results show a significant improvement with respect to the prediction obtained by the unconstrained ANN reported in Figure 3. The model is now able to predict correctly the directivity pattern: the magnitude and direction of the main lobes are accurately predicted. A noticeable error can be observed on the smaller lobes. However, this prediction error can be reduced by increasing the sampling of the database. This can be verified by comparing the results in Figure 5a, 5b and 5c which are obtained by using 6, 11 and 21 sampling frequencies for the generation of the training database. As the database is enriched, the order of the polinomial $\mathrm{I}_p(\log(f))$ is increased: polynomials with order 5,6 and 8 are used for the databases with 6, 11 and 21 sampling frequencies, respectively.

A similar behaviour is observed for a prediction at a lower frequency. In Figure 6 a prediction at frequency $f = 220$ Hz is shown. This case is not included in the training database, the closest values being 199.53 Hz and 251.19 Hz. Also in this case, the prediction error can be reduced by increasing the number of sampling of frequencies for the generation of the training database (Figures 6a, 6b and 6c).

Comparing the two cases, $f = 220$ Hz and $f = 4500$ Hz, it can be inferred that a more dense database is necessary to obtain a given accuracy when the frequency of the prediction is increased.

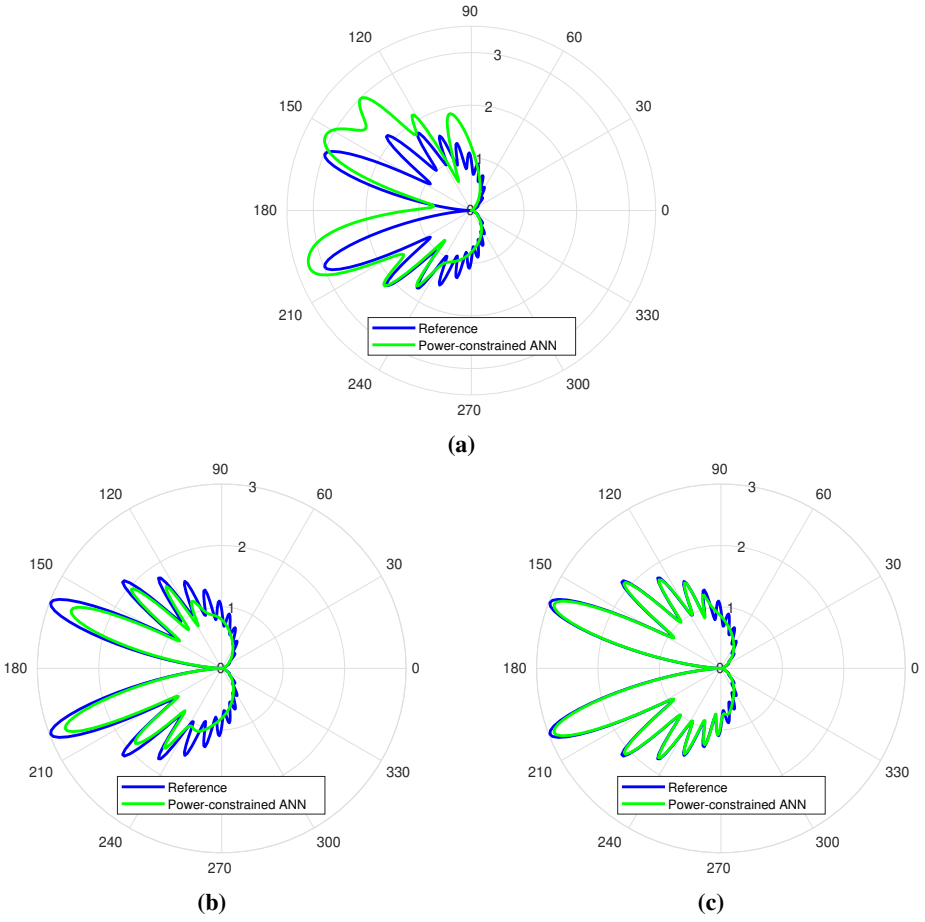

(a)

(b) (c)

Fig. 5 Directivity pattern predicted by power-constrained ANN at 4500 Hz: training database with 5(a), 10(b) and 20(c) frequency intervals

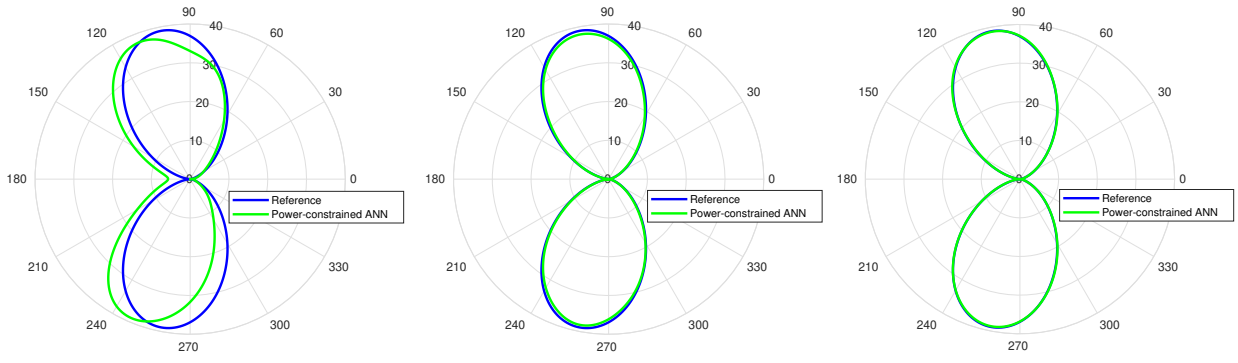

(a) (b) (c)

Fig. 6 Directivity pattern predicted by power-constrained ANN at 220 Hz: training database with 5(a), 10(b) and 20(c) frequency intervals

C. Power-constrained RF model

A similar approach is investigated for the RF model which is trained by the scikit-learn library [23]. Also in this case the database is pre-processed by normalising the $\mathcal{I}$ with respect to $\mathrm{I}(f)$ and the predictions are scaled with respect to the integral physical constraint

$$\mathcal{I}(\theta, f)_{RF} = \frac{\mathrm{I}_p(\log(f))}{\int_0^{2\pi} \tilde{\mathcal{I}}_{RF}(\theta', \log(f))d\theta'} \tilde{\mathcal{I}}_{RF}(\theta, \log(f)) \ . \tag{6}$$

The prediction at $f = 220$ Hz and $f = 4500$ Hz, obtained by a RF with 1000 trees and unlimited depth, are reported in Figures 7 and 8 respectively. The results show that the RF model is able to capture correctly the main trend in the data.

Furthermore, the RF algorithm offers the possibility to easily evaluate the prediction uncertainty. The square root of the variance between the predictions of the different trees in the forest can be used to estimate the uncertainty. For this reason, the plots show also a lower bound and an upper bound for the prediction. This feature of RF is quite useful when dealing with small databases in which only few reference points are available.

Comparing Figures 5a and 8a , it can be inferred that the RF method, with respect to the ANN method, is able to better capture the main features of the physical problem, the sound directivity , even in the case of a coarse database. Moreover, RF is able to recover the structure of the low intensity lobe, while the ANN model is always inaccurate, even using the largest database.

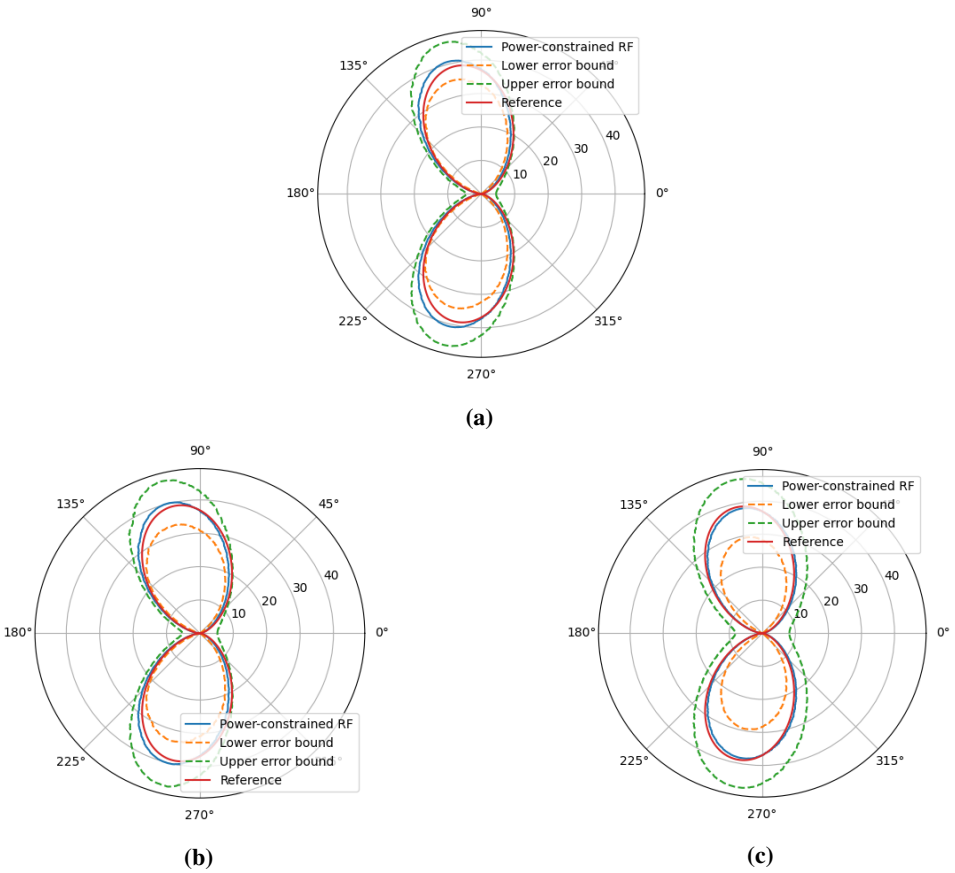

Fig. 7 Directivity pattern predicted by power-constrained RF at 220 Hz: training database with 5(a), 10(b) and 20(c) frequency intervals

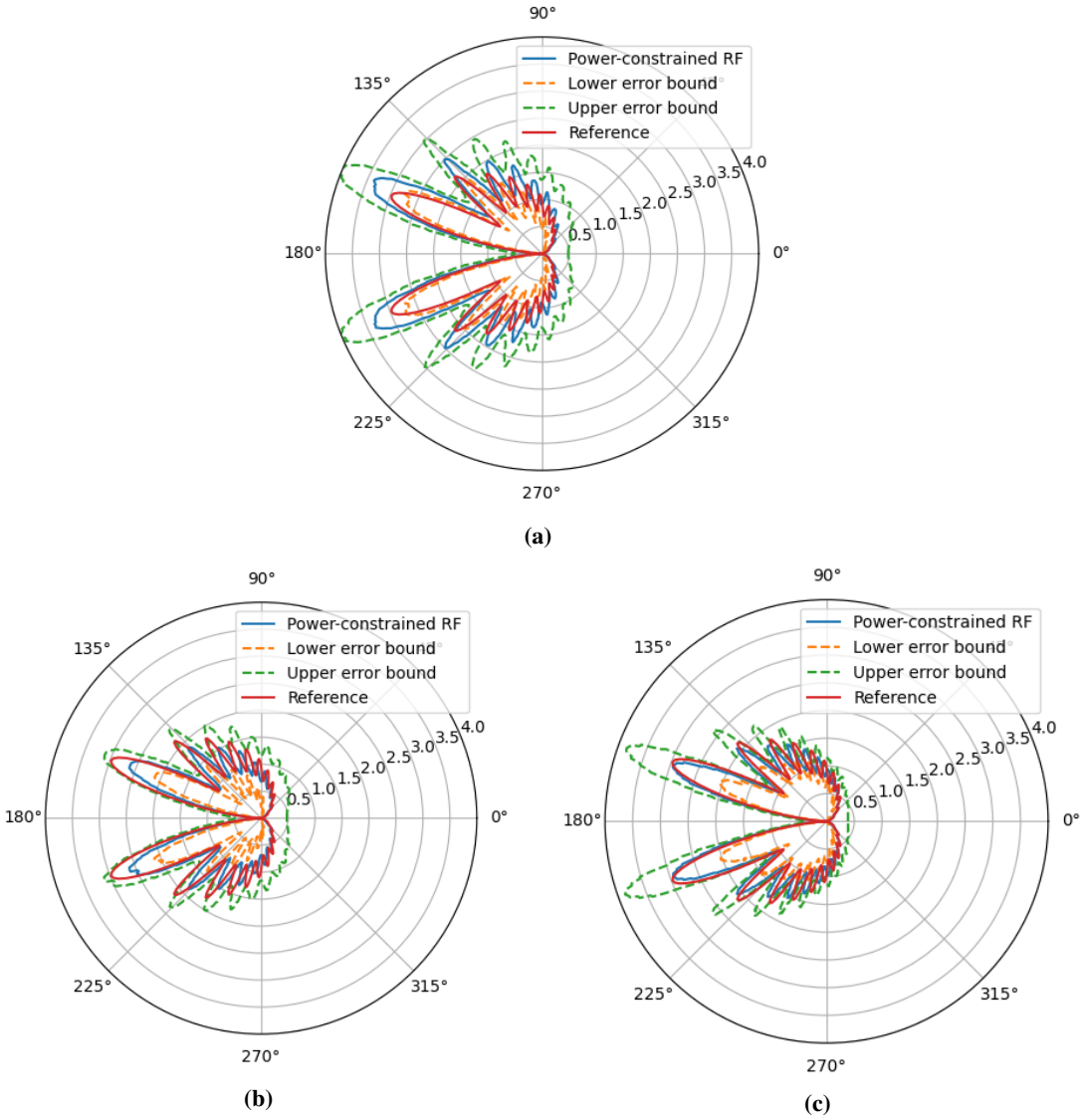

(a)

(b)

(c)

Fig. 8 Directivity pattern predicted by power-constrained RF at 4500 Hz: training database with 5(a), 10(b) and 20(c) frequency intervals

IV. Conclusion

Two machine learning data-driven methods, one based on a standard feed-forward Artificial Neural Network (ANN), with sigmoid activation functions, and one based on Random Forest (RF) algorithm, were applied to far-field directivity data sets of the trailing-edge noise. The goal of the present work is to evaluate the predictive ability of the ANN and RF models to mimic the complex pattern of the far-field directivity for a wide range of frequencies.

The proposed procedure was tested on an artificial database generated by the Amiet model, assuming that the model is able to represent the fundamental features of the trailing-edge noise problem: this artificial database represents a good benchmark for testing the predictive capability of the data-driven models. However, the data-driven models can be directly trained on available experimental data or high-fidelity calculations: in this way the simplifications required by the Amiet model can be avoided and the approach can be applied to general configurations since the proposed methodology does not require any particular assumption on the shape of the body.

The proposed models are based on a splitting in sub models: the ANN or the RF algorithm is used to describe the noise directivity while a polynomial model is introduced for the prediction of the emitted acoustic power. This splitting improved significantly the training performance and can be interpreted as a possible way to introduce a physical constraint to the machine learning model which is forced to satisfy a constraint on the emitted power.

Both methods were able to accurately represent the complex directivity patterns. From this preliminary investigation it can be inferred that the RF method, with respect to the ANN method, is able to better capture the main features of the physical problem, the sound directivity, even in the case of a coarse database. Moreover, RF is able to recover the structure of the low intensity lobe, while the ANN model with the chosen architecture is always inaccurate, even using the biggest database. It would be possible to further increase the complexity of the ANN and this could improve the prediction of the low intensity lobes: however, the training of the ANN tested in this work is significantly more expensive than the training of the chosen RF architecture. Furthermore, the potential of RF regression for the evaluation of the prediction uncertainty was also addressed.

References

[1] Howe, M. S., "Trailing Edge Noise at Low Mach Number," *J. Sound Vib.*, Vol. 225(2), 1999, pp. 211–238.

[2] Brooks, T. F., Pope, D. S., and Marcolini, M. A., "Airfoil Self-Noise and Prediction," Tech. rep., NASA RP 1218, 1989.

[3] Amiet, R., "Noise Due to Turbulent Flow Past a Trailing Edge," *J. Sound Vib.*, Vol. 47(3), 1976, pp. 387–393.

[4] Amiet, R., "Effect of Incident Surface Pressure Field on Noise Due to Turbulent Flow Past a Trailing Edge," *J. Sound Vib.*, Vol. 57, No. 2, 1978, pp. 305–306.

[5] Grasso, G., Jaiswal, P., Wu, H., Moreau, S., and Roger, M., "Analytical Models of the Wall-pressure Spectrum Under a Turbulent Boundary Layer with Adverse Pressure Gradient," *J. of Fluid Mechanics*, Vol. 877, 2019, p. 1007–1062.

[6] Goody, M., "Empirical Spectral Model of Surface Pressure Fluctuations," *AIAA Journal*, Vol. 42, No. 9, 2004, p. 1788–1794.

[7] Roger, M., and Moreau, S., "Back-scatterng Correction and Further Extensions of Amiet's Trailing-edge Noise Model. Part 1: Theory," *J. Sound Vib.*, Vol. 286, 2005, pp. 477–506.

[8] Rozemberg, Y., Robert, G., and Moreau, S., "Wall-pressure Spectral Model Including the Adverse Pressure Gradient Effects," *AIAA J.*, Vol. 50, No. 12, 2012, pp. 2168–2179.

[9] Kamruzzaman, M., Bekiropoulos, D., Lutz, T., Wurz, W., and Kramer, E., "A Semi-empirical Surface Pressure Model for Airfoil Trailing-edge Noise Prediction," *Int. J. Aeroacoustics*, Vol. 14, 2015, pp. 833–882.

[10] Lee, S., "Empirical Wall-pressure Spectral Modeling for Zero and Adverse Pressure Gradient Flows," *AIAA J.*, Vol. 56, No. 5, 2018, pp. 1818–1829.

[11] Hu, N., "Empirical Model of Wall Pressure Spectra in Adverse Pressure Gradients," *AIAA J.*, Vol. 56, No. 9, 2018, pp. 3491–3506.

[12] Brunton, S. L., Noack, B. R., and Koumoutsakos, P., "Machine Learning for Fluid Mechanics," *Ann. Rev. of Fluid Mechanics*, Vol. 52, 2020, pp. 477–508.

[13] Duraisamy, K., Iaccarino, G., and Xiao, H., "Turbulence Modeling in the Age of Data," *Ann. Rev. of Fluid Mechanics*, Vol. 51, 2019, pp. 357–377.

[14] Goodfellow, I., Bengio, Y., and Courville, A., *Deep Learning*, MIT Press, 2016.

[15] Hastie, T., Tibshirani, R., and Friedman, J., *The Elements of Statistical Learning: Data Mining, Inference and Prediction*, Second Edition, Springer, 2009.

[16] Wilsby, O. L., and Sandberg, R. D., "Data-Driven RANS Closures for Trailing Edge Noise Predictions," *25th AIAA/CEAS Aeroacoustics Conference*, 2019, p. 2444.

[17] Dominique, J., Christophe, J., Schram, C., and Sandberg, R. D., "Inferring Empirical Wall Pressure Spectral Models with Gene Expression Programming," *J. Sound Vib.*, Vol. 506, 2021, p. 116162.

[18] Herr, M., Ewert, R., Rautman, C., Kamruzzaman, M., Bekiropoulos, D., Arina, R., Iob, A., Batten, P., Chakravarthy, S., and Bertagnolio, F., "Broadband trailing-edge noise predictions overview of BANC-III results," *21st AIAA/CEAS Aeroacoustics Conference*, 2015, p. 2847.

[19] Glegg, S., and Devenport, W., *Aeroacoustic of Low Mach Number Flows*, Academic Press, 2017.

[20] Roger, M., and Moreau, S., "Extension and Limitations of Analytical Airfoil Broadband Noise Models," *int. J. of Aeroacoustics*, Vol. 9, No. 3, 2010, pp. 273–305.

[21] Drela, M., "An analysis and design system for low Reynolds number airfoils," *Low Reynolds Number Aerodynamics*, Springer-Verlag, 2015.

[22] Arina, R., and Ferrero, A., "Data-Driven Modeling of Broadband Trailing-Edge Noise," *27th Int. Congress on Sound and Vibration*, 2021.

[23] Pedregosa, F., Varoquaux, G., Gramfort, A., Michel, V., Thirion, B., Grisel, O., Blondel, M., Prettenhofer, P., Weiss, R., Dubourg, V., Vanderplas, J., Passos, A., Cournapeau, D., Brucher, M., Perrot, M., and Duchesnay, E., "Scikit-learn: Machine Learning in Python," *Journal of Machine Learning Research*, Vol. 12, 2011, pp. 2825–2830.